ELSEVIER

Nuclear Instruments and Methods in Physics Research A 485 (2002) 615–623

NUCLEAR INSTRUMENTS & METHODS IN PHYSICS RESEARCH Section A

www.elsevier.com/locate/nima

Optimization of a ^{6}LiF bolometric neutron detector

C.S. Silver[a,c,1], J. Beeman[b], L. Piccirillo[d], P.T. Timbie[a,*], J.W. Zhou[c,2]

[a] *Department of Physics, University of Wisconsin, 1150 University Ave., Madison, WI 53706, USA*
[b] *Haller-Beeman Associates, Inc., 5020 Santa Rita Rd., El Sobrante, CA 94803, USA*
[c] *Princeton Optronics, Inc., 196 Princeton-Hightstown Rd., Princeton Junction, NJ 08550, USA*
[d] *Department of Physics and Astronomy, University of Wales - Cardiff, Wales, CF24 3YB, UK*

Received 9 February 2001; received in revised form 27 August 2001; accepted 25 October 2001

Abstract

The optimization of a ^{6}LiF bolometer for neutron spectroscopy applications has been accomplished with a series of 12 different detectors. This type of detector is similiar to X-ray bolometers, which have been extensively studied, and the absorber has a high neutron capture cross-section. Each bolometer was irradiated with alpha particles to investigate its response to thermal pulses. The best resolution obtained with this series of bolometers was 39 keV FWHM at 5.3 MeV. One of the bolometers was calibrated with monoenergetic neutrons, and its thermal properties are derived from measurements over a range of temperatures. We discuss the considerations involved in optimizing a ^{6}LiF bolometer for different types of neutron applications.

Keywords: Neutron; Neutron spectroscopy; Bolometers; Calorimeters; Detectors

1. Introduction

The bolometric spectroscopy of particles enables energy resolution limited only by thermodynamic fluctuations and detection efficiency determined by the reaction cross-section of the absorbing crystal. For example, monolithic silicon microcalorimeters have been used to obtain 4.5 eV resolution for 6 keV X-rays [1], close to the theoretical limit for a practical detector of 2 eV FWHM at an energy of 10 keV [2]. For an ideal bolometer, the theoretical resolution is given by $\Delta E(\mathrm{FWHM}) = 2.355\zeta\sqrt{kT^2C}$ [3], where T is the detector temperature, C is the bolometer's total heat capacity, and ζ is a dimensionless constant generally between 1 and 2 which depends on the thermistor's sensitivity. Massive bolometers with large efficiencies have been built for detecting weakly interacting particles. The CDMS dark matter experiment reported 650 eV FWHM resolution at 10 keV using a 165 g high-purity germanium crystal [4].

High resolution neutron spectroscopy can facilitate research in nuclear science, materials characterization, and dosimetry, and it can provide critical information about nuclear fission and fusion reactions [5]. Additionally, neutron spectroscopy has important applications in explosives detection [6]. Conventional neutron spectrometers employing ^{3}He and ^{6}Li utilize either

*Corresponding author.
E-mail address: timbie@wisp.physics.wisc.edu (P.T. Timbie).

[1] Currently at Glimmerglass Networks, 26142 Eden Landing Rd., Hayward, CA 94545, USA.

[2] Currently at ADP/OMR Systems, 101 Business Park Dr., Skillman, NJ 08558, USA.

0168-9002/01/$ - see front matter
PII: S0168-9002(01)02146-5

neutron-induced nuclear reactions or elastic neutron scattering by light nuclei, with characteristic resolutions at 1 MeV of 20% and 5%, respectively. Solid-state semiconductor detectors obtain resolutions near 2% but have counting efficiencies below 10^{-5}, and they are inadequate for applications involving weak neutron sources. By comparison, a typical bolometer for neutrons operating at 0.4 K has a theoretical resolution at 1 MeV of 0.1% with an efficiency near 1%. Bolometers have more than an order of magnitude better energy resolution and detection efficiency compared to competing technologies.

This paper reports on the development of a series of ^{6}LiF composite bolometers and their optimization for single particle neutron spectroscopy applications. A bolometer is a thermal radiation detector consisting of an absorbing element in thermal contact with a thermistor. The absorber converts incident radiation to heat and the thermistor measures the resulting temperature rise. The heat then passes through a weak thermal link to a thermal bath. Overviews of bolometer theory and considerations in optimizing bolometer performance can be found in [2,7,8]. In designing a bolometer for neutron detection, it is important to consider both energy resolution and counting rate. Theoretically a bolometer's resolution $\Delta E \sim \sqrt{C}$, which indicates that a smaller total volume will provide superior resolution. The thermistor's sensitivity can also affect the resolution of a bolometer. A semiconductor thermistor has a characteristic sensitivity $\alpha = -\mathrm{d}(\ln R)/\mathrm{d}(\ln T)$ which determines the amplitude of its response to a thermal pulse at a given temperature. The counting rate is determined by the bolometer's efficiency, which is maximized with a large detector volume. Additionally, the counting rate is limited by the detector's decay time constant which scales as $\tau \approx C/G$ where G is the dominant thermal conductivity between the absorber and the heat sink. This suggests that a smaller detector volume can be preferable for applications involving large neutron fluxes. All of these considerations motivated the iterative development of 12 bolometers for the purpose of studying the optimal design for neutron spectroscopy.

In this work we exploit the ^{6}Li(n,α)t reaction. The Q-value for the reaction is 4.782 MeV [9], and the cross-section at 1 MeV is 0.312 b, falling to 0.095 b at 4 MeV [10]. ^{6}LiF was chosen for these detectors because it is a crystalline form of ^{6}Li, which has a high capture cross-section for neutrons. The high Debye temperature of ^{6}LiF means that it has low heat capacity at a given temperature, and this allows a significant response to thermal pulses. A fast neutron incident on a ^{6}LiF bolometer is captured by this reaction and the alpha and triton are absorbed in the crystal, resulting in a temperature rise corresponding to the total energy of the neutron plus the Q-value. For thermal neutrons the reaction products are emitted in opposite directions after the absorption with a range of 50 μm, and for 4 MeV neutrons the maximum range of the two particles is less than 0.7 mm. Thermal neutrons were detected with this reaction by de Marcillac et al. using a 2 g LiF bolometer operated at 80 mK [11]. Tests of this detector with alpha particles showed 16 keV resolution at 5 MeV. More recently, a massive enriched LiPb bolometer at 4 K has been used to measure large fluxes of thermal neutrons, taking advantage of the high cross-section for thermal neutrons [12].

2. Detectors and instrumentation

A summary of the 12 detectors that were tested is given in Table 1. Each bolometer consisted of a ^{6}LiF absorber attached to a thermistor and suspended from a copper mount which was in thermal contact with a cold stage. Cubic crystals of LiF grown by the Stockbarger method and enriched to 99.99% ^{6}Li were purchased from Bicron [13] in sizes ranging from 0.032 to 1 cm^3. With the exception of bol.03, the suspension was constructed using tensioned nylon fibers running across two faces of the absorber and epoxied onto the mount. A different type of suspension consisting of Delrin tubes of low thermal conductivity was tested with the bol.03 series of bolometers. Each end of the Delrin tube was fitted with a spring which provided compression against the absorber and the copper mount. Bol.01 through

Table 1
Summary of the detector parameters. Distinct bolometers are labeled by numbers, and modifications to these bolometers are indicated by letters

Name	^{6}LiF size (mm^3)	Suspension	NTD thermistor, attachment	Thermal link
Bol.01	$4 \times 4 \times 2$	Nylon fiber	D, epoxy	Leads
Bol.01a		Nylon fiber	D, epoxy	Leads + additional wire
Bol.02	$6 \times 6 \times 6$	Nylon fiber	D, epoxy	Leads
Bol.02a		Nylon fiber	F, epoxy	Leads
Bol.02b		Nylon fiber	F, epoxy	Leads + additional wire
Bol.03	$6 \times 6 \times 6$	Delrin tube	D, epoxy	Leads
Bol.03a		Delrin tube	F, epoxy	Leads + additional wire
Bol.03b		Rebuilt delrin tube	F, epoxy	Leads + additional wire
Bol.04	$6 \times 6 \times 6$	Nylon fiber	F, indium solder	Leads
Bol.05	$6 \times 6 \times 6$	Nylon fiber	F, indium solder	Leads + additional wire
Bol.06	$10 \times 10 \times 10$	Nylon fiber	F, indium solder	Leads
Bol.07	$6 \times 6 \times 6$	Nylon fiber	G, indium solder	Leads

bol.03 had drops of Miller–Stephenson epoxy [14] attaching the LiF crystal to the nylon suspension. Later bolometers had drops of epoxy on the nylon to hold the crystal in place, but no epoxy on the crystal itself.

Each thermometer consisted of a neutron transmutation doped (NTD) p-type Ge thermistor purchased from Haller–Beeman Associates, Inc. [15]. Doping concentrations of Ga and compensating As for thermistor types D, F, and G were, respectively (in units of 10^{16} cm^{-3}): 4.5 Ga, 1.3 As; 3.6 Ga, 1.0 As; 6.1 Ga, 1.7 As. Typical values of T_0 for these thermistors were, respectively, 44, 56, and 25 K, and therefore type F had the highest sensitivity and type G had the lowest. The geometry of the thermistors was selected such that their resistance at the operating temperature was several MΩ. Gold contact pads were deposited on both sides of the wafer, and then each chip was cut to $500 \times 500 \times 250$ μm^3. The electrical leads consisted of copper wire 50 μm in diameter, and they also served as a thermal link between the absorber and the heat sink. For several bolometers another wire provided additional thermal conductivity in order to reduce the decay time constant.

Detectors bol.01 through bol.03 were fabricated by attaching the thermistor and thermal link wire to the absorber near an edge of the crystal with EPO-TEK H20E epoxy [16], and the electrical leads were epoxied to the thermistor. Bol.04 through bol.07 were constructed without any epoxy in direct contact with the absorber or its thermal link to the heat sink. For these detectors, 200 Å of titanium followed by 4000 Å of gold were deposited in a 2 mm × 2 mm patch at the center of the ^{6}LiF crystal's bottom face. The thermistor was then indium soldered to the Ti/Au patch, and the electrical leads were indium soldered to gold contacts on the thermistor. Fig. 1 shows the mounting schematic for this type of bolometer. The additional thermal link for bol.05 was indium soldered to the Ti/Au and then epoxied to the copper mount.

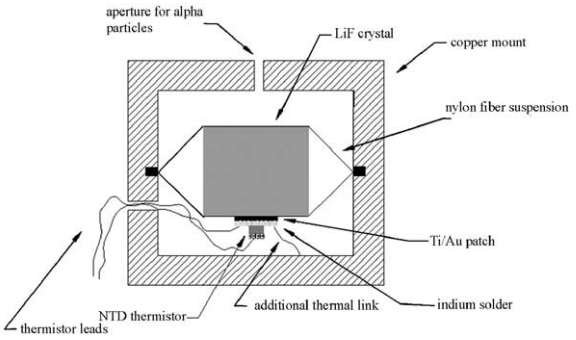

Fig. 1. Schematic of bol.04's mounting configuration, not drawn to scale. There are a total of 4 nylon support fibers, 2 as shown and 2 at 90^0 (not shown).

Most of the testing was performed at a heat sink temperature of 0.33 K using a single-stage ^{3}He refrigerator in contact with a pumped ^{4}He reservoir (based on [17]). For testing bol.04,

bol.06, and bol.07, temperatures as low as 0.1 K were obtained by mounting the detector on the cold finger of an adiabatic demagnetization refrigerator (ADR) [18]. The ADR provided reliable temperature stability between 0.1 and 0.7 K, enabling a characterization of the detectors' performance as a function of temperature.

The bolometers were biased at constant current through a load resistor in thermal contact with the copper mount. The bias circuit was powered by lithium batteries which provided a low-noise bias source without significant voltage drifts. Depending on the resistance of the thermistor at the bias point, the load resistors were $R_{\mathrm{load}} = 10\ \mathrm{M}\Omega$ (type D thermistor) or 20 MΩ (types F and G). The first stage of amplification was provided in the dewar by an NJ32 JFET which was thermally isolated from the ^{4}He stage by a G-10 fiberglass tube and heated to 100 K [19]. Outside the dewar the signal was further amplified and filtered with an analog bandpass filter. Each pulse was subsequently digitized and stored for off-line processing. Pulse height spectra were then generated by applying a least-squares fit to each pulse to determine the peak, using a simple model for the detector's rise and decay time constants. Unwanted pulses resulting from pile-up, microphonic noise, and background radiation were rejected using a chi-squared threshold, a baseline rms noise criterion, and a pulse height criterion.

3. Response to thermal pulses

Each detector was tested at ~ 0.3 K (with the exception of bol.07, which was optimized for operation at 150 mK) with a 0.1 uCi ^{210}Po alpha source mounted in front of the bolometer's aperture to measure the resolution and time constants for 5.3 MeV thermal pulses. These measurements are summarized in Table 2. Pulse heights doubled and decay time constants were reduced when the epoxy bonding the thermistor to the absorber was replaced by an indium Ti/Au interface (bol.04 through bol.07). This may be attributed to the relatively larger heat capacity and smaller thermal conductivity of epoxy. It has been reported [20,21] that phonon focusing in a cubic crystal concentrates the ballistic heat flux from a point source of phonons onto the center of the crystal's faces, which suggests that a thermistor centered on a face can collect phonons more efficiently than one placed near an edge of the crystal. Although detectors bol.04 through bol.07 were fabricated with face-centered thermistors, it is not possible to distinguish the effect of phonon focusing from that of thermal conductivity and heat capacity since all of these parameters were changed simultaneously.

There is a distinct trend toward lower pulse amplitudes and longer decay time constants in larger detectors, which can be understood as

Table 2
Bolometer response to alpha particles. Resolution is for the 5.3 MeV ^{210}Po alpha line. Rms noise was taken with no filtering in the amplifier electronics. The bol.03 series was highly sensitive to microphonics, and the rms noise quoted for those detectors was calculated from relatively quiet sections of data

Name	T_{bath} (mK)	Pulse height (μV)	Rms noise (μV)	S/N	Resolution (keV FWHM)	τ_{rise} (μs)	τ_{decay} (ms)
Bol.01	366	43	—	—	71	150	17.0
Bol.01a	328	227	0.698	325	39	80	3.1
Bol.02	328	65	0.890	73	170	200	11.6
Bol.02a	309	38	0.281	135	100	175	10.2
Bol.03	328	28	0.500	56	225	210	83.0
Bol.03a	325	32	0.367	87	193	450	10.8
Bol.03b	328[a]	24	0.917	26	—	650	10.0
Bol.04	328[a]	> 49	0.274	179	78	150	6.6
Bol.05	328[a]	37	0.190	195	118	165	4.3
Bol.06	328	32	0.306	105	—	160	26.0
Bol.07	150	62	0.752	82	—	430	5.5

[a] Thermometry was uncertain for these tests, but the bath temperature is most likely the base temperature of the ^{3}He refrigerator.

resulting from an increase in heat capacity due to the crystal. Bol.07 is identical to bol.04 except that it was fabricated with a type G thermistor, and its sensitivity is optimal near 0.2 K. With the same detector geometry, the lower temperature produces a significantly larger pulse amplitude and smaller decay time constant, suggesting that the resolution of these detectors in this temperature region is limited by their heat capacity. This trend is confirmed by the large pulse height and short decay time of the much smaller bol.01a.

All of the bolometers were sensitive to microphonic effects which resulted both from the absorber's support structure and from the high-impedance wiring between the bolometer and the JFET. To address this problem, the bol.03 series of bolometers were mounted with a stiffer suspension consisting of Delrin tubes compressed with springs. Unfortunately, contrary to what was expected, the bol.03 detectors were significantly more sensitive to microphonic noise. Determining the proper spring tension demands a balance between the suspension's oscillation frequency and the differential thermal contractions of the ^{6}LiF crystal and the copper mount as they cool. However, rebuilding the suspension with modified springs did not reduce the detector's sensitivity to microphonics, and the tube-mount scheme was therefore abandoned in later designs.

Bol.04 was tested in the ADR at several temperatures in order to measure the detector's dominant heat capacity and thermal conductivity as a function of temperature. Decay time constants and pulse amplitudes from 5.3 MeV alpha particles were measured at bias temperatures ranging from 0.25 to 0.4 K, above which temperature the baseline noise began to dominate the pulses. Load curves were measured over a similar range of temperatures by varying the bias current and observing the thermistor's voltage response. The results of these tests are discussed in Section 5.

Due to the relatively small volume of its absorber, bol.01a had the best energy resolution and shortest time constant of all of the detectors. This type of detector is ideal for high resolution spectroscopy of large neutron fluxes. For applications involving weaker neutrons sources, the larger bol.06 is more practical because of its greater detection efficiency, and if the neutron flux is weak enough the detector's long time constant will not limit its counting rate. These results suggest that the nature of the application dictates which bolometer design is optimal.

4. Response to monoenergetic neutrons

For calibrating the detector, a flux of neutrons was produced at the University of Wisconsin tandem accelerator using the D(d, n)^{3}He reaction. With a Q-value of 3.269 MeV, this reaction is well-suited to producing monoenergetic neutrons at several MeV with a fixed energy and rate. The deuterium gas target (12.2 cm in length) was separated from the accelerator vacuum system by a 0.5 μm 99.95% purity nickel foil. The foil was supported by a curved brass mount with a 3 mm aperture, and it was able to withstand a pressure difference of greater than 0.5 atm.

Before entering the target cell, the deuterium beam passed through a 25 μm thick tantalum aperture 1 mm in diameter to ensure alignment along the axis of the deuterium target cell, which was maintained at 100 Torr throughout the calibration. The beam exiting the accelerator was tuned to 1.000 MeV, and there was an energy loss in the foil of 57 keV. After passing through the target the deuterium beam was stopped by a 0.1 mm gold foil, and neutrons exited the target cell along its axis through 15 μm of aluminum. The target cell was electrically isolated from the accelerator, which enabled a measurement of the beam current directly at the far end of the target. The beam current was integrated for the duration of the experiment to measure the total charge that traversed the deuterium gas. A polypropylene window 250 μm thick was mounted on the dewar to minimize scattering in front of the detector, and strips of thin aluminized mylar were used as radiation shields for the 300, 77, and 4 K stages of the dewar. The sides of the dewar were surrounded with a $\frac{1}{16}''$ thick borated cadmium shield to reduce the rate from thermal neutrons in the room during the experiment.

The bolometer bol.04 was selected for calibration due to its combination of significant

signal-to-noise ratio and short thermal decay time constant. The detector was located 11 cm from the far edge of the target cell, at 0° to the axis of the beam. At this energy the neutron flux is strongly concentrated in the forward direction, and the spread in neutron energy across the active area of the detector is <1 keV. The energy of neutrons emitted from the target cell is a function of the deuterium beam energy, which degrades along the length of the target due to energy losses in the gas. There is no straightforward formula which can be used to calculate the neutron energy distribution from a thick target, so the resulting neutron energy and flux were calculated using successive thin target approximations. With a differential cross-section of 24 mb/ ster [22,23] for 1 MeV deuterons incident on deuterium gas, the calculated neutron spectrum at the detector consists of a sharp peak at 3.955 MeV at a rate of 61.3 neutrons/s, corresponding to a flux of 848 cm^{-2} s^{-1}.

As an independent measurement of the neutron flux generated in the target cell, an aluminum sample located directly in front of the target cell was activated, and the resulting gamma radiation was counted with a $3'' \times 3''$ right cylindrical NaI scintillation spectrometer contained in a lead shield 4″ thick to reduce background counts. The 10 min half-life of the $^{27}Al(n,p)^{27}Mg$ reaction made it convenient to irradiate the sample for 30 min, bringing it to 90% of its saturation activity, and then count the gamma decays for 10 min. Inscattering was minimal for 4 MeV neutrons due to the 3.8 MeV threshold of this reaction. Aluminum also reacts with neutrons by $^{27}Al(n,\alpha)^{23}Na$ with a 15 h half-life, and contamination due to that reaction was negligible. The activation test was repeated several times to reduce the error due to variations in the beam current, background radiation, and placement of the sample. Finally, the NaI detector was calibrated with a ^{60}Co gamma source of known activity to verify its intrinsic efficiency. This test resulted in a flux measurement at the location of the bolometer of 65 cm^{-2} s^{-1}, more than an order of magnitude lower than the flux calculated using $D(d,n)^3He$ cross-sections. The authors are not aware of an explanation for the reduced flux from the $D(d,n)^3He$ reaction. The bolometer itself measured a flux of 0.199 cm^{-2} s^{-1}, and using the neutron flux derived from the activation measurement, the resulting efficiency of 0.31% is consistent with the ^6Li neutron cross-section at 4 MeV of 0.1 b [10,24]. The bolometer's resolution for 3.955 MeV neutrons was 4.3%.

Bol.04 was also tested with 5 and 7 MeV neutrons in order to determine the linearity of its energy response. Superimposed spectra of alpha particles, thermal neutrons, and fast neutrons are shown in Fig. 2. This measurement showed a significant nonlinearity which scaled with energy. The discrepancy between linear response and observed response was 3% at 4 MeV. Marcillac et al. [11] report a 20% nonlinearity in a 2 g LiF bolometer operated at 80 mK, consistent with the crystal's change in internal energy on absorbing a particle. The condition for this type of linearity is $\Delta U_{\rm int}/U_{\rm int} = E/U_{\rm int} \approx \Delta T/T \ll 1$. For bol.04 $U_{\rm int} = 3$ GeV (determined from lattice vibrations with a Debye temperature of 730 K and $T_{\rm bolometer} = 0.38$ K), corresponding to an intrinsic 0.42% nonlinearity for 4 MeV neutrons, a factor of 10 below what is observed. However, additional electrical tests indicated that there was a voltage-dependent nonlinearity at the $\sim$ 2% level due to capacitance in the dewar wiring, so the detector's

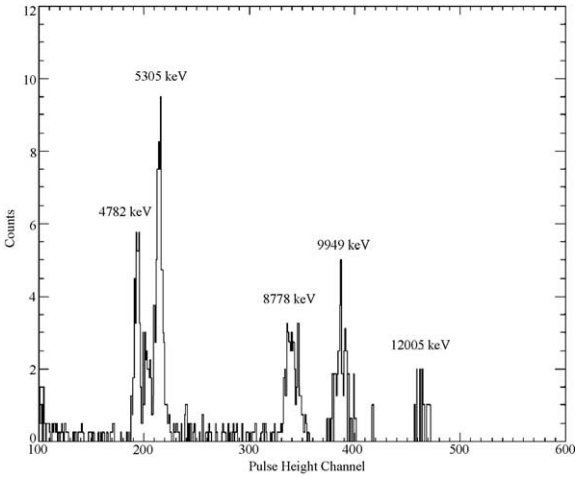

Fig. 2. Superimposed pulse height spectra of thermal neutrons, 5305 keV alpha particles, and monoenergetic fast neutrons at 3996, 5167, and 7223 keV. The labeled energies are the total energy deposited in the bolometer. Each spectrum is normalized to the exposure time of the 7223 keV neutrons.

linear energy response is consistent with the upper limit set by its internal energy.

5. Discussion

Detector bol.04's resolution and decay time constant are near the middle of the range for the whole series of detectors, so it was chosen for a more detailed study of its thermal properties. The expected heat capacity of bol.04 is modeled by summing the theoretical contributions from each material. The detector's heat capacity budget at 380 mK is listed in Table 3. It should be noted that the entire volume of the components that connect the absorber to the heat sink is included in the calculation, and therefore the total heat capacity is an upper limit. The dominant heat capacity results from the ^{6}LiF crystal, the copper leads, and the beads of Miller–Stephenson epoxy which hold the crystal in place against the nylon fiber suspension. Measurements of pulse amplitudes from alpha particles were used to estimate the detector's heat capacity given the temperature characteristics of the thermistor. The thermistor's sensitivity, $\alpha = -\mathrm{d}(\ln R)/\mathrm{d}(\ln T)$, determines its response to a small temperature rise at a given bias temperature, and for Ge thermistors $R = R_0 e^{\sqrt{T_0/T}}$ so $\alpha = -1/2T\sqrt{T_0/T}$($T_0 = 72.5$ K for bol.04). Since the detector's total heat capacity is given by $C = E_{\mathrm{alpha}}/\Delta T$, the heat capacity can be derived from thermal pulses using $C = \frac{1}{2} E_{\mathrm{alpha}}\, IR/\Delta V\sqrt{T_0/T^3}$, where ΔV is the drop in the thermistor's voltage due to the temperature change. Like the theoretical model, the measured heat capacity follows a distinct T^3 dependence due to the dominant lattice contribution to the specific heats. However, this measurement is a factor of 2 higher than the theoretical prediction from the bolometer's materials. For instance, at 380 mK the measured heat capacity is 21.8 nJ K^{-1}, whereas the predicted value is 11.2 nJ K^{-1}. It is unlikely that this discrepancy is due to systematic error in measuring α because it would require a factor of 4 in T_0 produce such a difference in heat capacity. While there is no clear explanation for this effect, excess heat capacity has been observed previously in an experiment with composite bolometers [25].

The detector's decay time constant, $\tau \approx 10$ ms, is independent of temperature, which suggests that the thermal conductivity between the absorber and the mount has the same temperature dependence as the heat capacity. For a bolometer biased at constant current with bias resistance R_L, electrothermal feedback results in an effective thermal conductivity $G_p = -\dfrac{\alpha P}{T}\dfrac{R_L - R}{R_L + R}$, where P is the bias power applied to the thermistor. This effective thermal conductivity contributes to the time constant $\tau = \dfrac{C}{G + G_p}$ [26]. In this case, τG_p is small

Table 3
Heat capacity budget for bol.04 at 380 mK

Material	C_v electron (J cm^{-3} K^{-2})	C_v lattice (J cm^{-3} K^{-4})	Volume (cm^3)	C (380 mK)(nJ K^{-1})
LiF [30]	—	4.9×10^{-7}	0.216	6.3
Ge [31][a]	1.9×10^{-7}	3.0×10^{-6}	6.3×10^{-5}	0.015
Ti [32]	3.2×10^{-4}	2.4×10^{-6}	8.0×10^{-8}	0.0097
Au [32]	7.2×10^{-5}	2.5×10^{-4}	1.6×10^{-6}	0.066
In(s) [33]	—	1.6×10^{-4}	1.6×10^{-6}	0.014
Cu [32]	9.7×10^{-5}	6.7×10^{-6}	8.1×10^{-5}	3.0
Nylon [34]	—	2.6×10^{-5}	3.9×10^{-7}	0.0069
Miller–Stephenson epoxy[b] [35]	$C_V = 1.27 \times 10^{-5} T^{1.3}$	J g^{-1} K^{-1},	0.5 mg	1.8
TOTAL				11.2

[a] This reference measures Ge with a higher doping concentration, and it is listed here to show that the lattice contribution dominates the specific heat.

[b] Modeled as a heavily filled epoxy, similar to EPO-TEK H20E.

compared with C, so G_p has little effect on the time constant. With the measured heat capacity and time constant, we estimate $G \approx 4 \times 10^{-5} T^3$ W K^{-1}. This is significantly lower than expected from the individual thermal conductivities of the bolometer's components, but it is consistent with measurements of the Kapitza mismatch at a metal–dielectric interface [27–29].This can be attributed to the thermal resistance at the boundary between the ^{6}LiF and the Ti/Au.

In principle, the detector's load curves constitute a straightforward and independent means to measure the thermal conductivity between the thermistor and the heat sink. However, it is seen from the load curves that a very large change in power results in a commensurately small change in thermistor temperature, and the load curves seem to suggest an exponential dependence on temperature that is larger than that of elecron–phonon decoupling. Additionally, load curves taken at different bath temperatures are inconsistent with one another. The thermal conductivity derived from the time constants seems to be more plausible than the one extracted from load curves, and we conclude that conduction from the absorber to the heat sink is limited by Kapitza resistance.

Given bol.04's measured heat capacity, the theoretical limit on its energy resolution at 0.4 K due to thermodynamic fluctuations is $\Delta E \approx 2$ keV, independent of the bolometer's thermal link. At this temperature, bol.04's measured resolution of 78 keV FWHM at 5.3 MeV is more than an order of magnitude above this. The measured baseline rms noise is consistent with the total noise expected from phonon and Johnson noise in the thermistor (27 keV), input noise of the JFET (30 keV), and a small contribution from microphonic noise. These sources of noise put a lower limit on the detector's resolution of ≈ 65 keV, close to the measured resolution. This suggests that there are no additional significant noise effects in the absorber. Both phonon noise and Johnson noise can be reduced by lowering the temperature, so in principle the detector's resolution may be limited by amplifier noise. It will be beneficial to perform a comprehensive study of composite ^{6}LiF bolometers at temperatures below 0.1 K in order to determine the ultimate limit on resolution for this type of detector. Since Kapitza resistance limits this bolometer's thermal conductivity, it seems that the only way to further improve the detector's resolution and counting rate simultaneously is to develop a larger bolometer for use at lower temperatures.

In conclusion, we constructed a variety of bolometric neutron detectors using ^{6}LiF as the absorber. We obtained pulse height spectra from the bolometers using alpha and neutron sources. For 4 MeV neutrons, we measured an efficiency of 0.31% and a resolution of 4.3%.

Acknowledgements

The authors wish to thank Lynn Knutson and Tom Finnessey for their help with the calibration measurements using the University of Wisconsin tandem accelerator. The detector development program was initiated by Junwei Zhou at Princeton Optronics, Inc., under DOE Award #DE-FG02-97ER82462. We also thank Karl Pitts for helpful discussions about neutron detector calibration and Dan McCammon for discussions about calorimetry.

References

[1] K.D. Irwin, G.C. Hilton, J.M. Martinis, S. Deiker, N.F. Bergren, S.W. Nam, D.A. Rudman, D.A. Wollman, Nucl. Instr. Meth. A 444 (2000) 184.
[2] D. McCammon, R. Almy, E. Apodaca, S. Deiker, M. Galeazzi, S.I. Han, A. Lesser, W. Sanders, R.L. Kelley, S.H. Moseley, F.S. Porter, C.K. Stahle, A.E. Szymkowiak, Nucl. Instr. Meth. A 436 (1999) 201.
[3] S.H. Moseley, J.C. Mather, D. McCammon, J. Appl. Phys. 56 (5) (1984) 1257.
[4] D.S. Akerib, et al., Nucl. Phys. B (Proc. Suppl.) 70 (1999) 64.
[5] A.J. Peurrung, Nucl. Instr. Meth. A 443 (2000) 400.
[6] R.A. August, G.W. Phillips, S.E. King, J.H. Cutchin, Nucl. Instr. Meth. A 352 (1994) 712.
[7] P.L. Richards, J. Appl. Phys. 76 (1) (1994) 1.
[8] J.W. Zhou, P. de Marcillac, N. Coron, S. Wang, H.H. Stroke, O. Redi, J. Leblanc, G. Dambier, M. Barthelemy, J.P. Torre, O. Testard, G. Beyer, H. Ravn, J. Magnin, Nucl. Instr. Meth. A 335 (1993) 443.
[9] F. Ajzenberg-Selove, T. Lauritsen, Nucl. Phys. A 490 (1988) 1.

[10] F. Gabbard, R.H. Davis, T.W. Bonner, Phys. Rev. 114 (1959) 201.
[11] P. de Marcillac, N. Coron, J. Leblanc, C. Bobin, I. Berkes, M. De Jesus, J.P. Hadjout, L. Gonzalez-Mestres, J.W. Zhou, Nucl. Instr. Meth. A 337 (1993) 95.
[12] J.M. Richardson, W.M. Snow, Z. Chowdhuri, G.L. Greene, IEEE Trans. Nucl. Sci. 45 (3) (1998) 550.
[13] Bicron Crystal Products, Washougal, WA 98671.
[14] Epoxy 907, Miller-Stephenson Chemical Company, Inc., Danbury, Conn. 06810.
[15] Haller-Beeman Associates, Inc., El Sobrante, CA 94803.
[16] EPO-TEK H20E, Epoxy Technologies Inc., Billerica, MA 01821.
[17] J.P. Torre, G. Chanin, Rev. Sci. Instr. 56 (2) (1984) 318.
[18] P. Timbie, G. Bernstein, P. Richards, Cryogenics 30 (1990) 271.
[19] Cooled JFET amplifier, IR Labs, Tucson, AZ 85719.
[20] D.C. Hurley, J.P. Wolfe, Phys. Rev. B 32 (4) (1985) 32.
[21] M.R. Hauser, R.L. Weaver, J.P. Wolfe, Phys. Rev. Lett. 68 (17) (1992) 2604.
[22] G.T. Hunter, H.T. Richards, Phys. Rev. 76 (10) (1949) 1445.
[23] H.A. Hussain, S.E. Hunt, Int. J. Appl. Radiat. Isot. 34 (9) (1982) 1363.
[24] M. Drosg, D.M. Drake, J. Masarik, Nucl. Instr. Meth. B 94 (1994) 319.
[25] D.C. Alsop, C. Inman, A.E. Lange, T. Wilbanks, Appl. Opt. 31 (1992) 6610.
[26] M. Galeazzi, Rev. Sci. Instr. 69 (5) (1998) 2017.
[27] A.C. Anderson, R.E. Peterson, Cryogenics 10 (1970) 430.
[28] A.E. Lange, E. Reysa, S.E. McBride, P.L. Richards, Int. J. Infrared Millimeter Waves 4 (5) (1983) 689.
[29] R.E. Peterson, A.C. Anderson, J. Low Temp. Phys. 11 (1973) 639.
[30] V.V. Panchenko, V.A. Yakovlev, Sov. Phys. Solid State 14 (1973) 2616.
[31] P.H. Keesom, G. Seidel, Phys. Rev. 113 (1959) 33.
[32] R.J. Corruccini, J.J. Gneiwek, N.B.S. Monograph, vol. 21, 1960.
[33] H.R. O'Neal, N.E. Phillips, Phys. Rev. A 137 (3) (1965) 748.
[34] W. Reese, J.E. Tucker, J. Chem. Phys. 43 (1) (1965) 105.
[35] S. Weyhe, B. Junge, F. Petzoldt, S. Bruns, W. Gey, Cryogenics 23 (1983) 166.